Title:

Sensitivity to geometric shape regularity in humans and baboons:

A putative signature of human singularity

Authors: Mathias Sablé-Meyer[1,2]*, Joël Fagot[3], Serge Caparos[4,5], Timo van Kerkoerle[1], Marie Amalric[6], and Stanislas Dehaene[1,2*].

Affiliations:

[1] Cognitive Neuroimaging Unit, CEA, INSERM, Université Paris-Saclay, NeuroSpin, Saclay, France

[2] Collège de France, Paris, France

[3] Laboratoire de Psychologie Cognitive ; CNRS & Aix-Marseille Université, Marseille, France

[4] Département de Psychologie, DysCo, Université Paris 8, Paris, France

[5] Institut Universitaire de France, Paris, France

[6] Carnegie Mellon University, Department of Psychology, Pittsburgh, PA, USA

*Correspondence to: mathias.sable-meyer@ens-cachan.fr or stanislas.dehaene@cea.fr

Abstract

Among primates, humans are special in their ability to create and manipulate highly elaborate structures of language, mathematics or music. Here, we show that this sensitivity to abstract structure is already present in a much simpler domain: the visual perception of regular geometric shapes such as squares, rectangles or parallelograms. We asked human subjects to detect an intruder shape among six quadrilaterals. Although the intruder was always defined by an identical amount of displacement of a single vertex, the results revealed a geometric regularity effect: detection was considerably easier when either the base shape or the intruder was a regular figure comprising right angles, parallelism or symmetry, than a more irregular shape. This effect was replicated in several tasks and in all human populations tested, including uneducated Himba adults and French preschoolers. Baboons, however, showed no such geometric regularity effect, even after extensive training. Baboon behavior was captured by convolutional neural networks (CNNs), but neither CNNs nor a variational auto-encoder captured the human geometric regularity effect. However, a symbolic model, based on exact properties of Euclidean geometry, closely fitted human behavior. Our results indicate that the human propensity for symbolic abstraction permeates even elementary shape perception. They suggest a new putative signature of human singularity, and provide a novel challenge for non-symbolic models of human shape perception.

Main Text

> [The universe] is written in mathematical language, and its characters are triangles, circles and other geometric figures, without which it is impossible to humanly understand a word.
>
> – *The Assayer*, Galileo Galilei

Among primates, humans are unique in their ability to develop formal symbolic systems that capture regularities in the external world, such as the language of mathematics. A great variety of non-exclusive hypotheses have been proposed to account for human singularity, including the emergence of evolved mechanisms for social competence (1), pedagogy (2), natural language (3, 4), or recursive structures across multiple domains such as language, music and mathematics (5–8). Unfortunately, few experimental paradigms, mostly in the domain of artificial grammar learning, afford a direct comparison of human and non-human primate behavior using the same methods (9–14). Here, we present experimental investigations of the differences between humans and baboons in the domain of geometry, and more specifically, the visual perception of quadrilaterals such a square, a rectangle or a parallelogram. We show that all humans, regardless of culture or education, are sensitive to the presence of geometric regularities such as right angles, parallelism or symmetry, and perform very differently from baboons in an elementary visual perception task.

Prehistorical records suggest that the human appeal for geometric shapes is as ancient as humanity itself. Circles, squares and spirals are omnipresent in human art and architecture.

The earliest engravings attributed to Homo sapiens, consisting of a triangular mesh of parallel lines, are estimated to be ~73000 years old (15). Even Homo erectus already drew abstract patterns ~540,000 years ago (16). Paleoanthropologists do not question the human origins of such drawings because, when given the opportunity to draw, other non-human primates never produce structured figures (17). By contrast, the diversity and abstraction of young children's drawings are striking (18, 19). Prior research has established that even preschoolers and adults with no formal education from the Amazon already possess sophisticated intuitions for geometry (20, 21) forming an intuitive mathematical "language of thought" (22). Those prior results suggest, but do not prove, that humans possess a much deeper level of understanding of the abstract properties of geometry than other primates. Here, our goal was to design a simple empirical test capable of probing this hypothesis.

We reasoned that if humans are spontaneously attuned to the major properties of Euclidean geometry (lines, length, parallelism, perpendicularity, symmetry) and their combinations, then they might exhibit a geometric regularity effect, with a better and faster perception of regular shapes, such as a square, than of irregular ones. Indeed, several previous experiments, both within and outside the domain of geometry, have shown that whenever regularities are present, humans use them to compress information in working memory and achieve a smaller "minimal description length", thus facilitating memorization, anticipation and outlier detection (22–26). Crucially, a shape perception test could be simple enough to probe the sensitivity of both human and non-human primates to the same mathematical properties. We opted for the intruder test, where a participant must simply find the outlier shape within a

set of six, and which has been previously used to explore human intuitions of geometry (20, 27).

Results

Design of the geometric intruder task. We selected 11 quadrilaterals ranging from perfect regularity (a square, with its four right angles, parallel lines and equal sides) to full irregularity (an arbitrary quadrilateral devoid of any of these properties) (Fig. 1A; exact shapes described in supplementary table T1). For each such reference shape, four deviant versions were generated by changing the position of the bottom-right vertex by a constant distance, either along the bottom side or along a circle centered on the bottom-left vertex (thus violating either distance or parallelism). All deviants departed from their reference shape by the same amount, and all 11 reference shapes were matched for average distances between vertices (see Supplementary Online Materials). On each trial of the intruder task, we selected one of the 11 possible reference shapes and presented five instances of it, varying in scale and orientation (e.g. 5 rectangles), together with a single deviant (in this case, a non-rectangle with the bottom-right vertex displaced). The location of this outlier was randomized, and six levels of shape rotation and shape scale were pseudo-randomly distributed among the six shapes. The participants' task was to click on the outlier shape, as fast and accurately as possible (figure 1B).

Intruder task in educated adults. In experiment 1, with N = 605 French adults, we observed a striking geometric regularity effect: error rates varied dramatically with the reference shape, from 2% to 40%, with a consistent ordering from regular to irregular (Fig. 1C; Univariate Type III Repeated-Measures ANOVA: $F(10, 6040) = 292.88$, $p < 10^{-15}$; explained variance evaluated by

the generalized eta squared: η^2_G= .27). By contrast, the size, rotation and position of the outlier had significant but only minor effects (size: F(5, 3020) = 4.46, p = .0005, η^2_G=.005; rotation: F(5, 3020) = 21.19, p < .0001, η^2_G=.021; position: F(5, 3020) = 4.96, p = .0001, η^2_G=.005). Response times were tightly correlated with error rates (linear regression: r^2 = .92, p < .0001) and therefore also exhibited a large geometric regularity effect (Fig. S1).

In experiment 1, the intruder was always a deviant shape, and was therefore more irregular than the reference shape. Thus, participants could have responded by selecting the most irregular among the six shapes on display. To avoid this confound, in experiment 2 and all subsequent experiments, half of the displays were canonical (five instances of one of the 11 reference shape, plus a single deviant) and half were swapped (five deviants, identical up to a rotation or scale change, plus a single reference shape; see examples in Fig. 1B). As previously, participants were simply asked to click on the shape that differed from the others. In a new group of N = 117 French adults, the geometric regularity effect was replicated (F(10, 1160) = 70.96, p < 10^{-15}, η^2_G=.25), while size, position and rotation effects again had either insignificant or very small effects (size: F(5, 580)=2.16, p=.056, η^2_G=.008 ; rotation: F(5, 580)=9.66, p < .0001, η^2_G=.031; position: F(5,580)=2.26, p=.047, η^2_G=.008). Response times also yielded a large geometric regularity effect (correlation with error rate: r^2=.95, p<.00001). Error rates were strongly correlated across experiments (r^2 = .97; p < 10^{-7}; Fig 1.D) and display types (r^2 = .84; p < .0001; Fig. 1.D).

Subjective ratings of complexity. Three additional experiments investigated the origins of the geometric regularity effect. First, we asked whether geometric regularity was cognitively

penetrable and could therefore be directly reported using subjective ratings. N = 27 French adults rated the subjective complexity and N = 21 rated the subjective regularity of each reference shape on a 1-100 scale. Both subjective ratings correlated tightly with error rates in the intruder task (complexity r^2=.88 and regularity r^2=.76; r^2=.84 after aggregating the two conditions by averaging complexity and 1 – regularity; all p<.0001; Fig. 1E). Since the early visual stages of object recognition are largely thought to be cognitively impenetrable (28), the finding that humans have correct intuitions that some geometric shapes are simpler than others suggesting that this effect arises at a level of representation beyond early vision.

Visual search. We further tested this idea by probing whether the search for geometric regularity engages parallel ("pop-out") or serial processes. N = 11 French adults engaged in a classic task of visual search for an outlier in arrays of 6, 12 or 24 shapes. Response times showed that search was always serial, for all 11 shapes, yet with a slope and an error rate that again correlated linearly with geometric regularity (p<.0001, r^2=0.98; Fig. 2; detailed analysis of the effects of number of items and item presence provided in Supplementary Materials). This finding shows that the regularity effect does not arise from an early pre-attentive pop-out, even for the simplest shapes such as square or rectangle. Rather, geometric shape perception involves an attention-dependent stage whose speed increases with geometric regularity.

Sequential presentation of shapes. As a further test of the perceptual stage at which the geometric regularity effect arises, we asked whether this effect would still be present if the shapes could not be perceived in one glance, but had to be mentally reconstructed for a sequential display of their vertices. N = 16 French adults participated in an experiment in which

the shapes were broken down into a sequence of four dots, one for each vertex location, in a systematic order. By having the sequence unfold over a time span of 1.8 s, thus largely exceeding the time window for integration within the ventral visual recognition system (29, 30), our goal was to prevent classical bottom-up shape recognition mechanisms, yet still allow subjects to grasp the geometric relationships between the 4 vertices. The experiment was run in small blocks, each with reference shapes. In the first six trials of a given block, the four dots always traced a fixed quadrilateral (e.g. rectangle), with variations in size and orientation. Then, on each subsequent trial, the first 3 dots continued to trace the same quadrilateral (again with variations in size and orientation), but on half of the trials the fourth dot was displaced to one of the four possible deviants shown in figure 1A. Participants were asked to indicate if the last dot was correctly or incorrectly located. Even under this sequential condition, the geometric regularity effect was replicated: the error rate still varied dramatically across shapes ($F(8, 120) = 10.1$, $p<10^{-9}$, $\eta^2_G=.16$) and the effect correlated with the geometric regularity effect observed for static shapes ($r^2 = .56$; $p = .02$; Fig. 1F). Thus, the effect arises from a level of representation where geometric properties can be ascertained even when they are not simultaneously present in the stimulus.

Probing the influence of education: Himbas and young children. We next investigated the dependence of the effect on age, education and culture. One possibility is that the effect arises from formal education in mathematics, for instance because regular shapes are also familiar, nameable, and taught at school. To address this concern, we turned to human populations with little or no formal schooling. First, we tested French preschoolers (N=28 kindergarteners; mean age 5 years 4 months; range 4:11 to 5:10 ; to shorten the duration of the experiment, children

were tested solely with canonical displays; N=156 1st graders were also tested, see supplementary materials and Fig. S2 for detailed results). Second, even since those Western children could have been introduced with shape names, we also tested 22 uneducated Himba adults, a pastoral people of northern Namibia whose language contains no words for geometric shapes, receive little or no formal education, and who, unlike French subjects, do not live in a carpentered world (31).

In both populations, the geometric regularity effect was replicated (Fig. 1G and 1H). In preschoolers, errors rates varied even more dramatically than in educated French adults across the 11 shapes. They remained below 20% for the square and rectangle, ~50% for the iso-trapezoid, and continued to climb up to 60-70% for more irregular quadrilaterals. The correlation of children and French adult performance was strong and remained significant even when excluding the two simplest shapes (square and rectangle; Fig. S2D). Similarly, the performance of Himba adults varied with geometrical regularity and was correlated with that of both French adults (r^2=0.55) and French preschoolers (r^2=0.59). Both findings converge with previous work (20, 22) to suggest that the geometric regularity effect reflects a universal intuition of geometry present in all humans and largely independent of formal knowledge, language, schooling, and environment.

Can baboon pass the intruder test? Next, we investigated whether the effect was also present in a non-human primate species, the guinea baboon (*Papio papio*). Baboons' visual system is largely similar to that of humans, and they perform similarly in some shape recognition tasks (e.g. ref *25*). We capitalized on a large facility where baboons can freely access testing booths

with touch screens (33). Twenty-six baboons received individualized training on the intruder task, using a great variety of images and textures (Fig. 3). Complete detail of each subject's learning history and performance is provided in Fig. S3 and in Supplementary Materials. A full data set was obtained from 20 animals who completed (1) an initial series of training stages on the intruder task with 10 non-geometric image pairs, progressively increasing in the number of available choices (Fig. 3A; 20 animals reached criterion; average of 5200 trials to criterion, range 1000 – 14500); (2) a first generalization to 10 novel non-geometric image pairs, indicating that they understood the intruder task (only tested in 18 animals; average = 272 trials, range 100 – 700); (3) a second generalization to black-and-white geometric shapes, where a simple non-geometric parameter sufficed to respond (e.g. pick a small triangle amidst large pentagons; average = 220 trials, range 100 – 600); and finally (4) generalization and further retraining with the complete set of quadrilaterals identical to human participants (average 6305 trials, range 704 – 8712).

Twenty of the 26 animals showed a clear understanding of the intruder task, because following training with 20 non-geometric images, they showed immediate first-trial generalization to new such images and/or to easily distinguishable polygons (Fig. 3B). However, when presented with the 11 quadrilaterals, baboons' performance collapsed, suggesting that they found all of them equally similar (Fig. 3C). Their performance was close to chance on the first test block (76.2% errors, SE=1%; chance = 83.3%) and slowly progressed on subsequent days. 11 animals continued performing the geometrical task for 8000 trials or more, eventually reaching 53% errors (significant deviation [SD]=6.7%) on blocks 81 to 99. Note that this performance was comparable to that of the preschoolers and 1st graders, who achieved

respectively 51% (SD=14%) and 48% errors (SD=16%). Yet even in the latter blocks, for the 11 primates who reached that stage and had therefore received consequent training, no geometric regularity effect was observed. Although error rates differed across the 11 shapes ($F(10, 100) = 24.68$, $p<10^{-14}$, .0001, $\eta^2_G=.44$), with a consistent ordering across baboons (Fig. S4), they correlated weakly and non-significantly with the geometric regularity effect found in human populations (Fig. 3C). Rather, their performances were impacted, at least in part, by visual properties that had little to no impact on our human participants, such as outlier rotation and outlier type (see table T2 for a systematic investigation of the significance and effect size of each predictor on each population). Thus, baboons performed poorly with quadrilaterals and were insensitive to their geometric regularities.

Models of human and baboon performance. To shed light on the dissociated performance of humans and baboons, we contrasted two classes of models of the intruder task (Fig. 4). The first class assumes that quadrilaterals are processed by standard image recognition mechanisms in the ventral visual pathway, while the second assumes an additional level of discrete, symbolic processing of non-accidental geometrical properties.

We modeled the ventral visual pathway using CORnet, one of the top-scoring convolutional neural networks (CNN) on brain-score.org, a platform that compares computational models with behavioral and neural observations (34) (other CNNs gave identical results; see Supplementary Online Materials). This model was pre-trained to label photographs on ImageNet, a large set of images featuring natural and man-made items. To determine if this model could successfully simulate the outlier task, we fed the network, without retraining, with

each of the six images actually presented to the participants on a given trial, collected the corresponding activation vectors in each CNN layer, and defined as the intruder the image whose vector differed most from the mean of the others. When averaging across trials, this process yielded a predicted error rate for each shape, separately for each layer in the model.

A second class of model, capitalizing on the prior demonstration of categorical perception for parallels and perpendicularity (27), assumes that quadrilaterals are mentally encoded as a symbolic list of discrete geometric properties. For each shape, the model loops over all pairs of sides and angles and generates a vector of 0's and 1's for the presence or absence of equal angles, equal sides, parallelism, and right angles (with a tolerance fitted to 12.5%, although this parameter had little impact, see Fig. S5). The difficulty of spotting the intruder is then predicted to be inversely related to the $\mathcal{L}_1$ distance between the symbolic vectors coding for the reference and deviant shapes.

Fig. 4C shows the matrix of correlation, over the 11 shapes, between the errors rates for each human population, each of the 11 well-trained baboons, and the predictions of the two models. Two squares are apparent. First, all baboons are intercorrelated, and their performance is well predicted by the last layer of the CNN model, putatively corresponding to ventral inferior temporal cortex (IT; mean across animals: r = .81, SE = .03). However, the CNN model is a poor predictor of human performance (mean across human groups: r = .48, SE = .10; the two distributions are significantly different: t-test, p = .024) and reaches significance only for Himbas and preschoolers (p = .005 and p = .048 respectively). Second, conversely, all human groups are well predicted by the symbolic model (mean r=.84, SE=.05, see table T3 for a

breakdown of the effect of each symbolic property), but that model is a poor predictor of baboon behavior (mean r = .44, SE = .04; the two distributions are significantly different: t-test, $p < .001$).

This double dissociation was confirmed by a two-parameter multiple regression where the predictions of the two models were put in competition to predict 44 data points (11 shapes x 4 deviants) per population (Fig. 4D). The three experiments with French adults who received formal education were almost exclusively captured by the symbolic regressor, and each baboon's data by the neural-network regressor. Interestingly, uneducated populations (Himba adults and French preschoolers) showed a significant contribution of both models.

Thus, the modelling suggests that two strategies are available to solve the intruder task and may coexist in humans (31, 35): an early visual capacity, shared with other non-human primates, to recognize shapes in the ventral visual pathway and use this code to detect a salient deviation in shape; and a higher-level universal human capacity to grasp abstract geometric properties. The former may exploit a variety of early and late visual cues, since further analysis of the CNN's performance showed some degree of predictability of the baboons' behavior by the V1 layer already, or by the surface area of the stimuli (Fig. S6). The abstract strategy, however, appears out of reach of such simple perceptual models (indeed, without further assumptions, the neural networks would have been incapable of passing the sequence version of the task, as humans did).

We verified that several other similar neural networks, such as DenseNet or ResNet, were similarly unable to fit human behavior (Fig. S7). It could be argued that the geometric

shape fell too far off the training space to elicit uninterpretable results. However, the model trained to label the ImageNet dataset did attribute to each geometry shape a highly consistent label (mostly “envelopes”; Supplementary Table T4). In order to test the effect of the training space, we modified the network with extra output units and trained it to label our reference shapes (Fig. S8). Four training strategies were tried, depending on whether we trained the network to label all 11 shapes or just the shapes with names in English; and whether all layers were allowed to change, or just the final layer (see Supplementary Materials). Nevertheless, all four manipulations failed to increase their predictive power of the CNN for any human population, and either worsened the predictive power for the baboon behavior, or left it unchanged. Since CNNs are far from perfect in capturing human behavior, even for natural stimuli(36–38), we also tested Variational Auto-Encoders(39) (VAE), whose architecture “compresses” information and may therefore be more suited to the task of encoding regular shapes. A classical VAE was successfully trained to encode and decode our reference shapes (Fig. S9A). However, it too did not exhibit the geometric regularity effect. First, its loss function varied very little across the 11 shapes (Fig. S9B). All shapes were learned similarly across training epochs, and the loss did not correlate well with either the human or the baboon behavior (Fig. S9C). Second, using the same methodology as for CNNs, we probed whether the internal compressed representation of the model could be used to spot the outlier; again, it proved to be predictive of neither the humans’ or the baboons’ behavior (Fig. S9D).

Discussion

Using the geometric intruder test, regardless of the human populations we tested, we observed a replicable geometric regularity effect: finding an intruder amongst six quadrilaterals is much easier when either the reference or the deviant shape are highly regular. This effect is already present in young children (preschoolers and 1st graders), and was also replicated in uneducated adults from a remote non-Western population with reduced access to education, suggesting that the effect does not depend on age, culture and education. Additionally, we show that this effect is replicable using different presentation modes (by presenting the entire shape at once, or the four vertices sequentially) and different tasks (intruder, serial search, or subjective complexity rating).

Given this apparent universality in humans, it is noteworthy that the baboons did not share this effect. Their performance was initially quite poor with all quadrilaterals, but even when it later improved to the level of human children and showed significant variations across shapes, it still did not correlate with the geometrical regularity effect. This striking difference occurred even though the baboons clearly understood the demands of the intruder task, having reached a threshold of 80% correct or more on a first set of stimuli (where chance is 16.7% correct) and then generalized to new non-geometrical stimuli. It also cannot come from a lack of motivation: while a few baboons did not complete the training, the twenty on which we collected data spontaneously performed an average of 867 geometrical trials per day (1st quartile 278 trials, median 641 trials, 3rd quartile 1332 trials).

An empiricist could argue that the difference was due to the different environments in which humans and baboons live. The “carpentered world” hypothesis (40) proposes that an

increased sensibility for right angles and parallel lines arises naturally from a Western style of life in a world full of rectilinear shapes (objects, buildings, books, etc.). Indeed, this was the dominant environment for most of our participants. However, several arguments refute this idea. First and foremost, the effect was present in the Himba people, but not in baboons. Yet the rural settlements of the Himba are quite unlike industrialized societies and their environment is relatively free of rectilinear objects. Conversely, the baboons we tested were not wild animals, but grew up and lived in an environment comprising a mixture of natural objects (trees and rocks) and man-made, rectilinear objects (buildings, doors, computer screen), which was arguably as "carpentered" as the Himbas' (see illustration in Supplementary Materials).

Second, even in a carpentered world, after projection in two dimensions, irregular shapes are arguably more frequent that regular ones on the retina, because the observers are rarely perfectly aligned with their environment for a rectilinear projection to occur. Parallelograms are also rare in our environment -- and yet they figured among the shapes with few errors. Thus, it is not clear how frequency in the environment would explain our result. Finally, we directly tested this empiricist hypothesis by training artificial neural networks with a dataset (ImageNet) that featured many man-made rectilinear image categories, such as envelopes, binders, band-aids or lampshades (labels which they readily applied to our quadrilaterals; see table T4). Even more crucially, we retrained them with our geometric shapes (see figure S8). Neither types of training sufficed for the neural networks to predict human behavior.

The dissociated performance of humans and baboons suggests that the intruder task can be solved using two strategies: a perceptual strategy, well captured by current neural-network models of the ventral visual pathway, in which geometric shapes are encoded using the same feature space also used to recognize any image (e.g. faces, objects, etc); and a symbolic strategy, in which geometric shapes are encoded by their discrete non-accidental regularities such as right-angles or parallel sides. The latter strategy seems available to all humans, whether in Paris or in rural Namibia. It is tempting to speculate that it may be available *only* to humans, as suggested by the failure of all the baboons we tested. At the moment, however, this proposal remains tentative, because we only tested a limited number of humans and a single non-human primate species. Both facets of this proposal will have to be submitted to further tests, for instance by contrasting human infants, who are known to be born with sophisticated symbolic abilities (41), and chimpanzees, who may lack a logical or hierarchical mode of data analysis (8).

The present results converge with prior research, using more complex geometric displays and tasks, which indicated that all humans, even young or uneducated ones, possess intuitions for geometry (20–22) and automatically apply a symbolic, language-like formalism to geometric data (22, 42). Brain imaging showed that this "language of geometry" rests primarily on dorsal and inferior sectors of prefrontal cortex (42). These regions are activated whenever humans reason about mathematical concepts and recombine them algebraically (43–45). While they are located outside of classical language areas, their surface area is strikingly expanded in the human lineage (46, 47), and they are therefore a good candidate for the emergence of novel human capacities in evolution, including symbolic mathematics. Previous work has shown

that proto-mathematical core knowledge is present in other non-human primates, such as numerosity in macaque monkeys (48, 49) or spatial navigation in baboons (50). However, what these species may be lacking is a capacity to discretize those representations and recombine them in larger language-like combinatorial expressions such as “four equal sides” (5–8), which are needed in order to conceive of a square and draw it. In the future, it would be informative to test whether chimpanzees who received “language training”, i.e. learned to use visual tokens to label numbers and objects (51, 52), would show the geometric regularity effect. There are reasons to doubt it, since careful analyses suggest that, unlike young children, chimpanzees do not use these tokens in productive combinations (11).

A parallel issue is, how could the neural networks we tested be modified to eventually pass the geometrical intruder test? Classical convolutional neural networks mimic only part of human visual recognition abilities (38). They roughly correspond to the first, bottom-up pass of invariant visual object recognition (53), but much more sophisticated recurrent top-down architectures are required to attain human-level performance in slower perceptual decision making tasks (54, 55). It will be interesting to examine if those newer models pass the present test or, as we tentatively suggest, if yet another level of symbolic representation, perhaps based on symbolic tree-based generative models and program inference (56–58), is needed.

In summary, the present results suggest a new putative human cognitive universal: the capacity to perceive the regularity of a geometric shape such as a square. They hint at the exciting possibility that humans differ from other primates in cognitive mechanisms that are much more basic than language comprehension or theory of mind, and involve a rapid grasp of

mathematical regularities in their environment. Those findings also provide a novel challenge for artificial intelligence, as none of the classical neural network models we tested so far could capture human behavior.

Materials and Methods

Reference shapes. All experiments relied on a single set of 11 fixed reference shapes, which were all quadrilaterals (Fig. 1A; the coordinates of their vertices are listed in Supplementary Table T1). We matched most reference shapes for two parameters. First, the average distance between all pairs of vertices (i.e., the mean of six distances) was the same across the 11 shapes. This ensured that the reference shapes had the same overall size. Second, the bottom edge was of fixed length across 9 of the 11 shapes – this was particularly important for the sequence experiment, where this segment was the last to appear on the screen and was the only one that could contain an outlier. The square and the rhombus were the only exceptions: they were only matched to other shapes on the average of distances. This was necessary because (1) the square had only one degree of freedom, and (2) the rhombus would otherwise have been either too similar to the square or utterly flat.

For some shapes (e.g. rectangle), this set of constraints led to a single choice for the specific shape. For others, we selected a shape that satisfied the constraints while being maximally different from the shapes in other categories. For instance, the specific quadrilateral that we selected for the “irregular” category made it maximally obvious that it did not have equal sides, parallel sides, equal angles or right angles.

The constraints that we adopted implied that the shapes were not strictly equalized in other dimensions such as surface or perimeter. Such residual differences might explain why the performance of neural networks and baboons varied slightly across shapes, but crucially they were uncorrelated with shape regularity (see Supplementary Materials).

Deviant shapes. For each reference shape, we generated four deviant shapes by changing the position of the bottom-right vertex. All deviant vertices were equidistant from the correct vertex location. Two deviant vertices were positioned along the bottom edge, either lengthening it or shortening it (see Figure 1A). The two other deviant positions preserved the correct distance from the bottom left vertex, and thus the length of the bottom edge, but changed its orientation. The distance of the deviant position from the correct position was fixed for all experiments and was common to all shapes. It was computed as a proportion of the (fixed) average distance between all pairs of vertices (55% for the sequence experiment; 30% for all other experiments).

Variations in orientation and size. In their default presentation, the shapes were centered on their center of mass, and their top vertex was horizontal. We then rotated the six shapes by a random permutation of the following angles: [-25°, -15°, -5°, 5°, 15°, 25°]. We avoided 0° rotation to prevent participants from relying on parallelism with the edges of the computer screen, and we avoided larger angles to side step the fact that some shapes had rotational symmetry (for instance, a 45° rotated square is identical to a -45° rotated square, but the same does not hold for a trapezoid). We also scaled the shapes by a random permutation of the following scaling factors: [0.875, 0.925, 0.975, 1.025, 1.075, 1.125].

Participants and experimental procedures. Details of the participants, design, procedure, and analyses specific to each experiment are presented as Supplementary Materials. Briefly, 612 French adults were recruited for online experiment 1, 117 for online experiment 2, and 48 for on-line subjective ratings. For the sequence and visual search experiments, we tested

respectively 16 and 11 participants in individual isolated testing booths. 28 French preschoolers (mean age 64 months; range 59-70 months; 15 boys, 13 girls) from two classrooms were tested individually in their school. Finally, 44 native Himba adults were recruited on-site in small individual villages of Northern Namibia (Southern Africa). All were monolingual native speakers of Otjihimba, a dialect of the Otjiherero language, which does not have vocabulary for most geometric shapes. Out of these, we report data for the 22 participants who did not attend a single year of schooling (for additional analyses of the effect of schooling, see Supplementary Materials).

Baboons (26 Papio papio, 18 females, age range 1.5-23 years, mean age 11 years) were tested at the CNRS primate facility (Rousset-sur-Arc, France). Baboons lived in a 700 m2 outdoor enclosure with access to indoor housing and could, on a voluntary basis, at any time, enter ten Automated Learning Devices for Monkeys equipped with a 19-inch touch screen, a food dispenser, and a radio-frequency identification (RFID) reader that could identify the animals

Data Availability

The data for all experiments is available on the Open Science Framework at https://osf.io/b7upd/?view_only=658848296a8a4c5d98b7a3d687373991

The code for the neural-network and symbolic models are provided at the same address, https://osf.io/b7upd/?view_only=658848296a8a4c5d98b7a3d687373991

References

1. E. Herrmann, J. Call, M. V. Hernandez-Lloreda, B. Hare, M. Tomasello, Humans Have Evolved Specialized Skills of Social Cognition: The Cultural Intelligence Hypothesis. *Science* **317**, 1360–1366 (2007).
2. G. Csibra, G. Gergely, Natural pedagogy. *Trends Cogn Sci* **13**, 148–53 (2009).
3. M. D. Hauser, N. Chomsky, W. T. Fitch, The faculty of language: what is it, who has it, and how did it evolve? *Science* **298**, 1569–79 (2002).
4. R. C. Berwick, N. Chomsky, *Why Only Us: Language and Evolution* (The MIT Press, 2016).
5. M. D. Hauser, J. Watumull, The Universal Generative Faculty: The source of our expressive power in language, mathematics, morality, and music. *Journal of Neurolinguistics* (2017) https:/doi.org/10.1016/j.jneuroling.2016.10.005 (January 28, 2017).
6. W. T. Fitch, Toward a computational framework for cognitive biology: unifying approaches from cognitive neuroscience and comparative cognition. *Phys Life Rev* **11**, 329–364 (2014).
7. S. Dehaene, F. Meyniel, C. Wacongne, L. Wang, C. Pallier, The Neural Representation of Sequences: From Transition Probabilities to Algebraic Patterns and Linguistic Trees. *Neuron* **88**, 2–19 (2015).
8. D. C. Penn, K. J. Holyoak, D. J. Povinelli, Darwin's mistake: explaining the discontinuity between human and nonhuman minds. *Behav Brain Sci* **31**, 109–30; discussion 130-178 (2008).
9. R. Malassis, S. Dehaene, J. Fagot, Baboons (Papio papio) Process a Context-Free but Not a Context-Sensitive Grammar. *Sci Rep* **10**, 7381 (2020).
10. L. Wang, L. Uhrig, B. Jarraya, S. Dehaene, Representation of Numerical and Sequential Patterns in Macaque and Human Brains. *Curr. Biol.* **25**, 1966–1974 (2015).
11. C. Yang, Ontogeny and phylogeny of language. *PNAS*, 201216803 (2013).
12. J. D. Smith, J. P. Minda, D. A. Washburn, Category learning in rhesus monkeys: a study of the Shepard, Hovland, and Jenkins (1961) tasks. *J Exp Psychol Gen* **133**, 398–414 (2004).
13. G. J. L. Beckers, R. C. Berwick, K. Okanoya, J. J. Bolhuis, What do animals learn in artificial grammar studies? *Neurosci Biobehav Rev* (2016) https:/doi.org/10.1016/j.neubiorev.2016.12.021.
14. S. Ferrigno, S. J. Cheyette, S. T. Piantadosi, J. F. Cantlon, Recursive sequence generation in monkeys, children, U.S. adults, and native Amazonians. *Science Advances* **6**, eaaz1002 (2020).
15. C. S. Henshilwood, *et al.*, An abstract drawing from the 73,000-year-old levels at Blombos Cave, South Africa. *Nature* **562**, 115–118 (2018).
16. J. C. Joordens, *et al.*, Homo erectus at Trinil on Java used shells for tool production and engraving. *Nature* **518**, 228 (2015).

17. A. Saito, M. Hayashi, H. Takeshita, T. Matsuzawa, The origin of representational drawing: a comparison of human children and chimpanzees. *Child Dev* **85**, 2232–2246 (2014).

18. F. L. Goodenough, Measurement of intelligence by drawings. (1926).

19. B. Long, J. Fan, Z. Chai, M. C. Frank, "Developmental changes in the ability to draw distinctive features of object categories" (PsyArXiv, 2019) https:/doi.org/10.31234/osf.io/8rzku (April 10, 2020).

20. S. Dehaene, V. Izard, P. Pica, E. Spelke, Core knowledge of geometry in an Amazonian indigene group. *Science* **311**, 381–384 (2006).

21. V. Izard, P. Pica, E. S. Spelke, S. Dehaene, Flexible intuitions of Euclidean geometry in an Amazonian indigene group. *Proc. Natl. Acad. Sci. U.S.A.* **108**, 9782–9787 (2011).

22. M. Amalric, *et al.*, The language of geometry: Fast comprehension of geometrical primitives and rules in human adults and preschoolers. *PLoS Comput. Biol.* **13**, e1005273 (2017).

23. R. N. Shepard, C. L. Hovland, H. M. Jenkins, Learning and memorization of classifications. *Psychological Monographs: General and Applied* **75**, 1–42 (1961).

24. J. Feldman, Minimization of Boolean complexity in human concept learning. *Nature* **407**, 630 (2000).

25. F. Mathy, J. Feldman, What's magic about magic numbers? Chunking and data compression in short-term memory. *Cognition* **122**, 346–362 (2012).

26. S. Planton, *et al.*, "Mental compression of binary sequences in a language of thought" (PsyArXiv, 2020) https:/doi.org/10.31234/osf.io/aez4w (October 28, 2020).

27. M. R. Dillon, M. Duyck, S. Dehaene, M. Amalric, V. Izard, Geometric categories in cognition. *Journal of Experimental Psychology: Human Perception and Performance* (2019) https:/doi.org/10.1037/xhp0000663.

28. Z. Pylyshyn, Is vision continuous with cognition?: The case for cognitive impenetrability of visual perception. *Behavioral and Brain Sciences* **22**, 341–365 (1999).

29. E. Greene, Information persistence evaluated with low-density dot patterns. *Acta Psychologica* **170**, 215–225 (2016).

30. J. Forget, M. Buiatti, S. Dehaene, Temporal integration in visual word recognition. *J Cogn Neurosci* **22**, 1054–68 (2009).

31. J. Davidoff, D. Roberson, L. Shapiro, Squaring the Circle: The Cultural Relativity of "Good" Shape. *J Cogn Cult* **2**, 29–51 (2002).

32. J. L. Fobes, J. E. King, *Primate behavior* (Academic Pr, 1982).

33. J. Fagot, E. Bonté, Automated testing of cognitive performance in monkeys: Use of a battery of computerized test systems by a troop of semi-free-ranging baboons (Papio papio). *Behavior Research Methods* **42**, 507–516 (2010).

34. M. Schrimpf, *et al.*, "Brain-Score: Which Artificial Neural Network for Object Recognition is most Brain-Like?" (Neuroscience, 2018) https:/doi.org/10.1101/407007 (February 8, 2020).

35. E. H. Rosch, Natural categories. *Cognitive psychology* **4**, 328–350 (1973).

36. N. Baker, H. Lu, G. Erlikhman, P. J. Kellman, Deep convolutional networks do not classify based on global object shape. *PLoS Comput Biol* **14**, e1006613 (2018).

37. R. Geirhos, *et al.*, ImageNet-trained CNNs are biased towards texture; increasing shape bias improves accuracy and robustness. *arXiv:1811.12231 [cs, q-bio, stat]* (2019) (October 26, 2020).

38. S. Ullman, L. Assif, E. Fetaya, D. Harari, Atoms of recognition in human and computer vision. *Proc Natl Acad Sci USA* **113**, 2744–2749 (2016).

39. D. P. Kingma, M. Welling, Auto-Encoding Variational Bayes. *arXiv:1312.6114 [cs, stat]* (2014) (October 26, 2020).

40. M. H. Segall, D. T. Campbell, M. J. Herskovits, Cultural Differences in the Perception of Geometric Illusions. *Science* **139**, 769–771 (1963).

41. G. Dehaene-Lambertz, E. S. Spelke, The Infancy of the Human Brain. *Neuron* **88**, 93–109 (2015).

42. L. Wang, *et al.*, Representation of spatial sequences using nested rules in human prefrontal cortex. *NeuroImage* **186**, 245–255 (2019).

43. M. Amalric, S. Dehaene, Cortical circuits for mathematical knowledge: evidence for a major subdivision within the brain's semantic networks. *Philos. Trans. R. Soc. Lond., B, Biol. Sci.* **373** (2017).

44. M. M. Monti, L. M. Parsons, D. N. Osherson, Thought beyond language: neural dissociation of algebra and natural language. *Psychol Sci* **23**, 914–922 (2012).

45. M. Maruyama, C. Pallier, A. Jobert, M. Sigman, S. Dehaene, The cortical representation of simple mathematical expressions. *NeuroImage* **61**, 1444–1460 (2012).

46. T. A. Chaplin, H.-H. Yu, J. G. M. Soares, R. Gattass, M. G. P. Rosa, A Conserved Pattern of Differential Expansion of Cortical Areas in Simian Primates. *Journal of Neuroscience* **33**, 15120–15125 (2013).

47. T. Xu, *et al.*, Cross-species functional alignment reveals evolutionary hierarchy within the connectome. *NeuroImage* **223**, 117346 (2020).

48. J. F. Cantlon, E. M. Brannon, Basic math in monkeys and college students. *PLoS biology* **5**, e328 (2007).

49. A. Nieder, S. Dehaene, Representation of number in the brain. *Annu Rev Neurosci* **32**, 185–208 (2009).

50. R. Noser, R. W. Byrne, Travel routes and planning of visits to out-of-sight resources in wild chacma baboons, Papio ursinus. *Animal Behaviour* **73**, 257–266 (2007).

51. T. Matsuzawa, Use of numbers by a chimpanzee. *Nature* **315**, 57–9 (1985).

52. D. Premack, "Minds with and without language" in *Thought without Language*, W. L., Ed. (Clarenton Press, 1988), pp. 46–65.

53. J. Kubilius, *et al.*, "CORnet: Modeling the Neural Mechanisms of Core Object Recognition" (Neuroscience, 2018) https:/doi.org/10.1101/408385 (February 8, 2020).

54. D. George, *et al.*, A generative vision model that trains with high data efficiency and breaks text-based CAPTCHAs. *Science* **358** (2017).

55. C. J. Spoerer, T. C. Kietzmann, J. Mehrer, I. Charest, N. Kriegeskorte, Recurrent neural networks can explain flexible trading of speed and accuracy in biological vision. *PLOS Computational Biology* **16**, e1008215 (2020).

56. J. Devlin, *et al.*, RobustFill: Neural Program Learning under Noisy I/O. *arXiv:1703.07469 [cs]* (2017) (October 26, 2020).

57. M. Balog, A. L. Gaunt, M. Brockschmidt, S. Nowozin, D. Tarlow, DeepCoder: Learning to Write Programs. *arXiv:1611.01989 [cs]* (2017) (October 26, 2020).

58. B. M. Lake, R. Salakhutdinov, J. B. Tenenbaum, Human-level concept learning through probabilistic program induction. *Science* **350**, 1332–1338 (2015).

Acknowledgements

This research was supported by a European Research Council (ERC) grant "NeuroSyntax" to S.D., as well as funding from INSERM, CEA, Collège de France and Fondation Bettencourt-Schueller. M.S.M. was supported by a doctoral grant from Ecole Normale Supérieure. The experiments on baboons were supported by labex BLRI (ANR-11-LABX-0036) and the Convergence ILCB institute (ANR-16-CONV-0002). S.C. was supported by Laboratoire Chrome, Université de Nîmes. We gratefully acknowledge help and feedback from Thomas Hannagan, Marie Lubineau, Cassandra Potier-Watkins, Bernadette Martins, Christine Doublé, Emmanuel Chemla, Véronique Izard, Anne Lurois at école maternelle Orry-la-Ville, Julie Gullstrand, Dany Paleressompoulle, the Unicog Lab, and the Département d'Etudes Cognitives of Ecole Normale Supérieure. We thank our research assistants, Chinho and Fanny, for their invaluable help, and the individual Himba for welcoming us and our project with openness, benevolence and generosity. We thank Jules Davidoff and Karina Linnell, who have made it possible for the Namibia data to be collected.

Author contributions

M.S. and S.D designed all experiments, analyzed the data and wrote the paper. J.F. designed and ran the experiment with baboons. S.C. ran the experiment with the Himba. T.v.K. and M.A. provided ideas and feedback on all experiments.

The authors declare no conflict interest.

List of Supplementary Materials

Supplementary Text; Figs. S1 – S9; Tables T1 – T4

Figure 1. Geometric regularity effect in humans

A, stimuli. We selected 11 quadrilaterals with various degrees of regularity, as defined by parallelism, equal sides, equal angles and right angles. For each quadrilateral, four deviants were generated by moving the bottom right corner by a fixed distance, thus shortening, lengthening or rotating the bottom side. **B, examples of intruder-task displays**. Left: circular display used in experiment 1. Participants had to tap the intruder. Center: Rectangular display used in experiment 2 and following. In the canonical presentation, five shapes exemplified a fixed quadrilateral, with variations in size and orientation, and the remaining shape was a deviant. In the swapped presentation, those two shapes were swapped. In either case, participants had to tap the intruder. Right: sequential presentation, unfolding from top to bottom and from left to right over the span of 1.8 seconds. Participants had to answer "correct" for properly placed dots (in green), and "incorrect" for deviant dots (example in red). **C, geometric regularity effect in experiment 1:** error rate varied massively with shape regularity in French adults. Shapes are ordered by performance and each is labeled with a color which is consistent across graphs. Error bars represent the standard error pooled over all participants – in this figure it is smaller than dot size. **D-H: Replications of the geometric regularity effect** with: **D**, swapped versus canonical trials in French adults; **E**, subjective judgments of shape complexity on a 1-100 scale; **F**, Sequential presentation of the four corners; **G**, French preschoolers; **H**, uneducated Himba adults from rural Namibia.

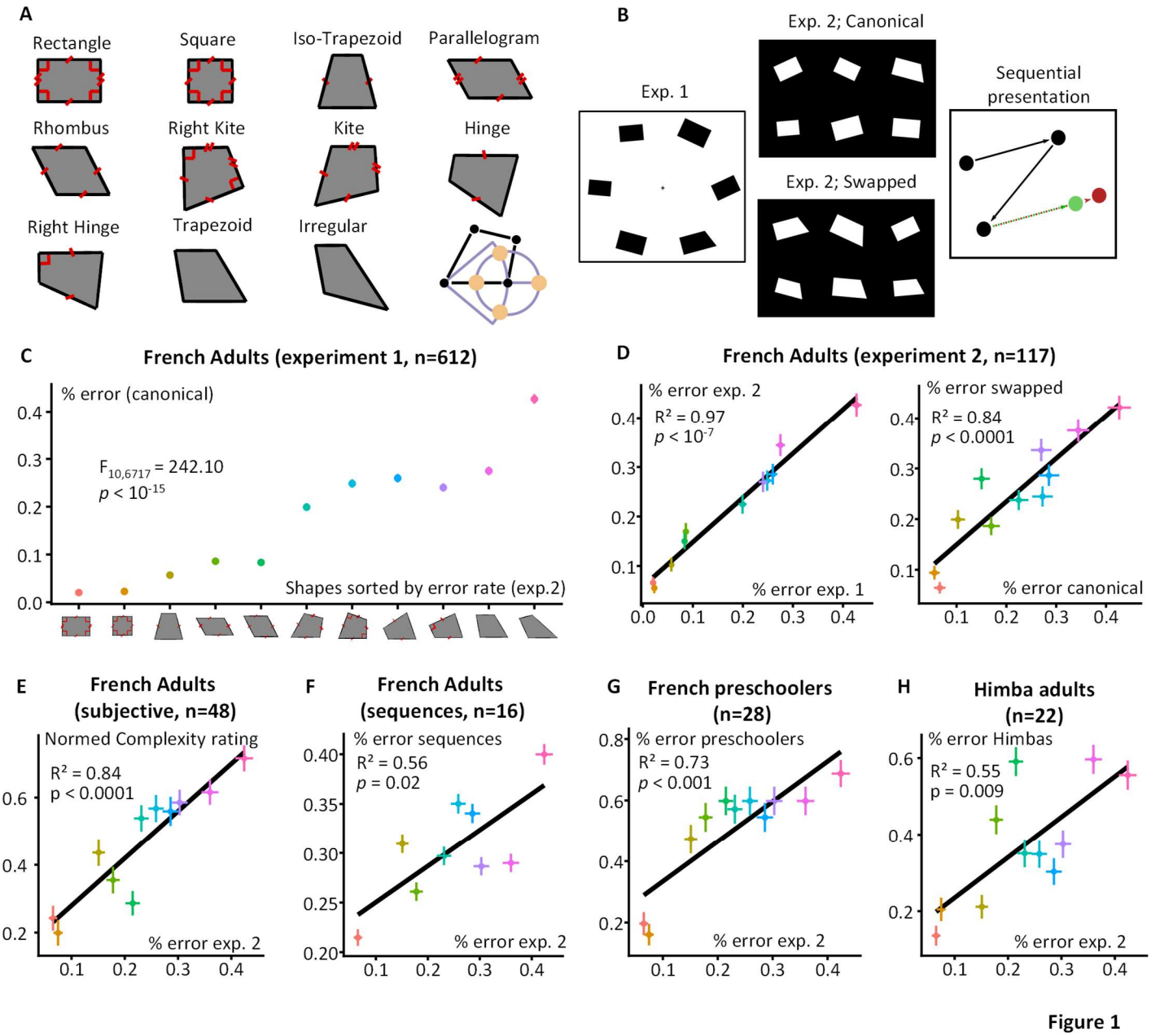
A
Rectangle
Square
Iso-Trapezoid
Parallelogram
Rhombus
Right Kite
Kite
Hinge
Right Hinge
Trapezoid
Irregular
B
Exp. 1
Exp. 2; Canonical
Exp. 2; Swapped
Sequential presentation
C
French Adults (experiment 1, n=612)
% error (canonical)
$F_{10,6717} = 242.10$
$p < 10^{-15}$
Shapes sorted by error rate (exp.2)
D
French Adults (experiment 2, n=117)
% error exp. 2
$R^2 = 0.97$
$p < 10^{-7}$
% error exp. 1
% error swapped
$R^2 = 0.84$
$p < 0.0001$
% error canonical
E
French Adults (subjective, n=48)
Normed Complexity rating
$R^2 = 0.84$
p < 0.0001
% error exp. 2
F
French Adults (sequences, n=16)
% error sequences
$R^2 = 0.56$
$p = 0.02$
% error exp. 2
G
French preschoolers (n=28)
% error preschoolers
$R^2 = 0.73$
$p < 0.001$
% error exp. 2
H
Himba adults (n=22)
% error Himbas
$R^2 = 0.55$
p = 0.009
% error exp. 2

Figure 1

Figure 2. Visual search paradigm. A, Examples of visual search displays. In the visual search task, 6, 12 or 24 shapes were randomly positioned inside a circle, and participant had to decide whether all the shapes were identical, irrespective of rotation and scaling, or whether there was one that differed from the others. They gave their binary present/absent response by pressing one of two possible keys on the keyboard. **B, Error rates in visual search task.** Errors rates increased with both the number of shapes and their complexity (geometric irregularity). The latter effect correlated tightly with the average error rate in the intruder task. **C, Search times. Left:** Slope of the visual search as a function of the number of displayed items, the presence or absence of an outlier, and the shape. **Right:** Correlation between the slope of the visual search on present trials and the error rates of the intruder task (exp. 2).

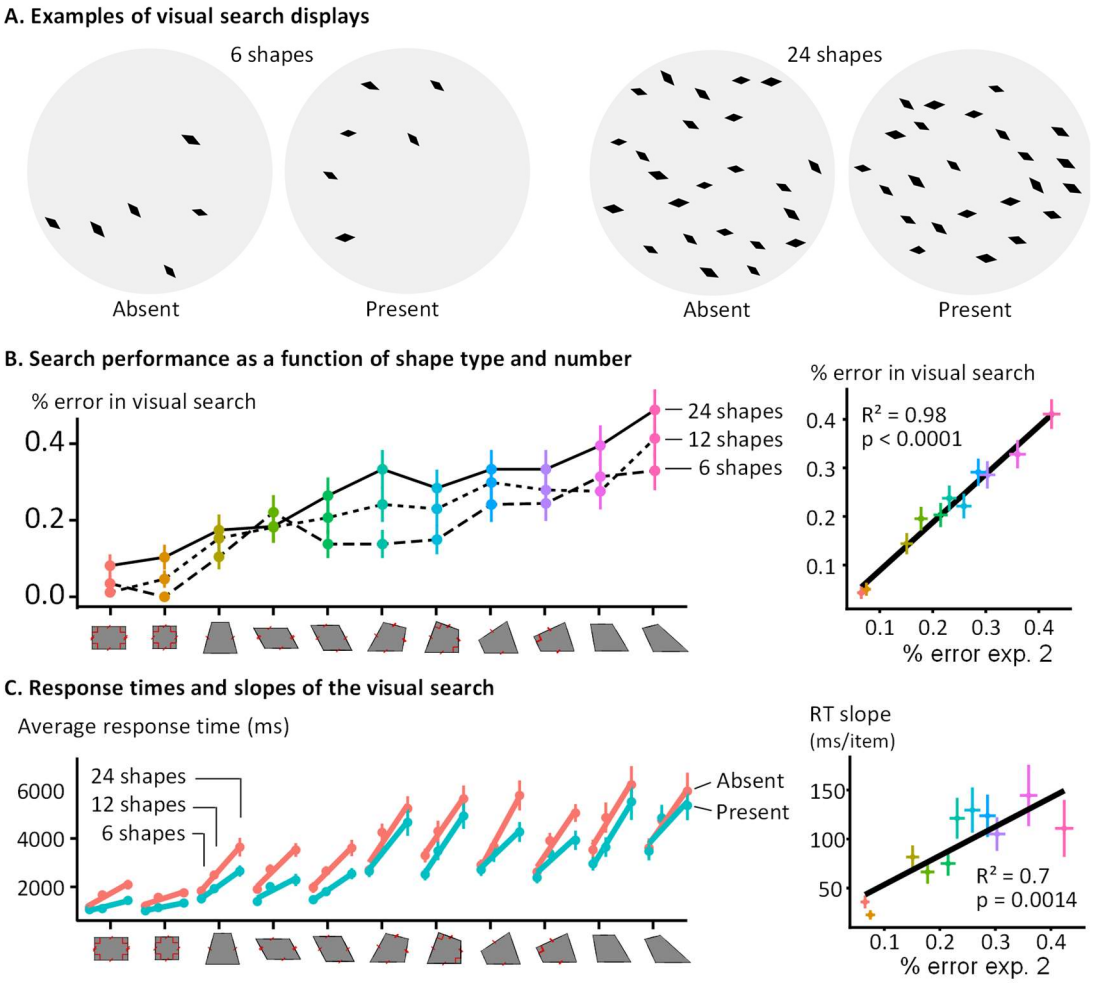

Figure 2

Figure 3. The geometric regularity effect is absent in baboons. A, training procedure. Each animal was trained for thousands of trials on the intruder task, first with a small number of fixed images (n=3, training stage 1), then with a larger number of images (up to 6, training stage 5) and with variations in size and orientation. Mastery of the task was verified through two generalization tests using novel images. Each baboon moved from one stage to the next only when the error rate fell below 20%. **B,** Summary of baboon training performance (first and last blocks of 88 trials each). Each color represents one baboon. Most animals attained criterion on the 10 pairs of shapes used for training (top) and successfully generalized to 10 new pairs of shapes (bottom left) and to 3 pairs of easily distinguishable polygons (bottom right; chance = 83.3% errors with 6 shapes). **C**, performance in the geometric intruder task. Left: average performance for each geometric shape at three stages: the first 33 test blocks, the middle 33 test blocks, and the last 33 test blocks. Each block contained 88 trials, and baboons took at most 99 blocks. Right: correlation between the average error rate in baboons and in French adults taking the same test (experiment 2).

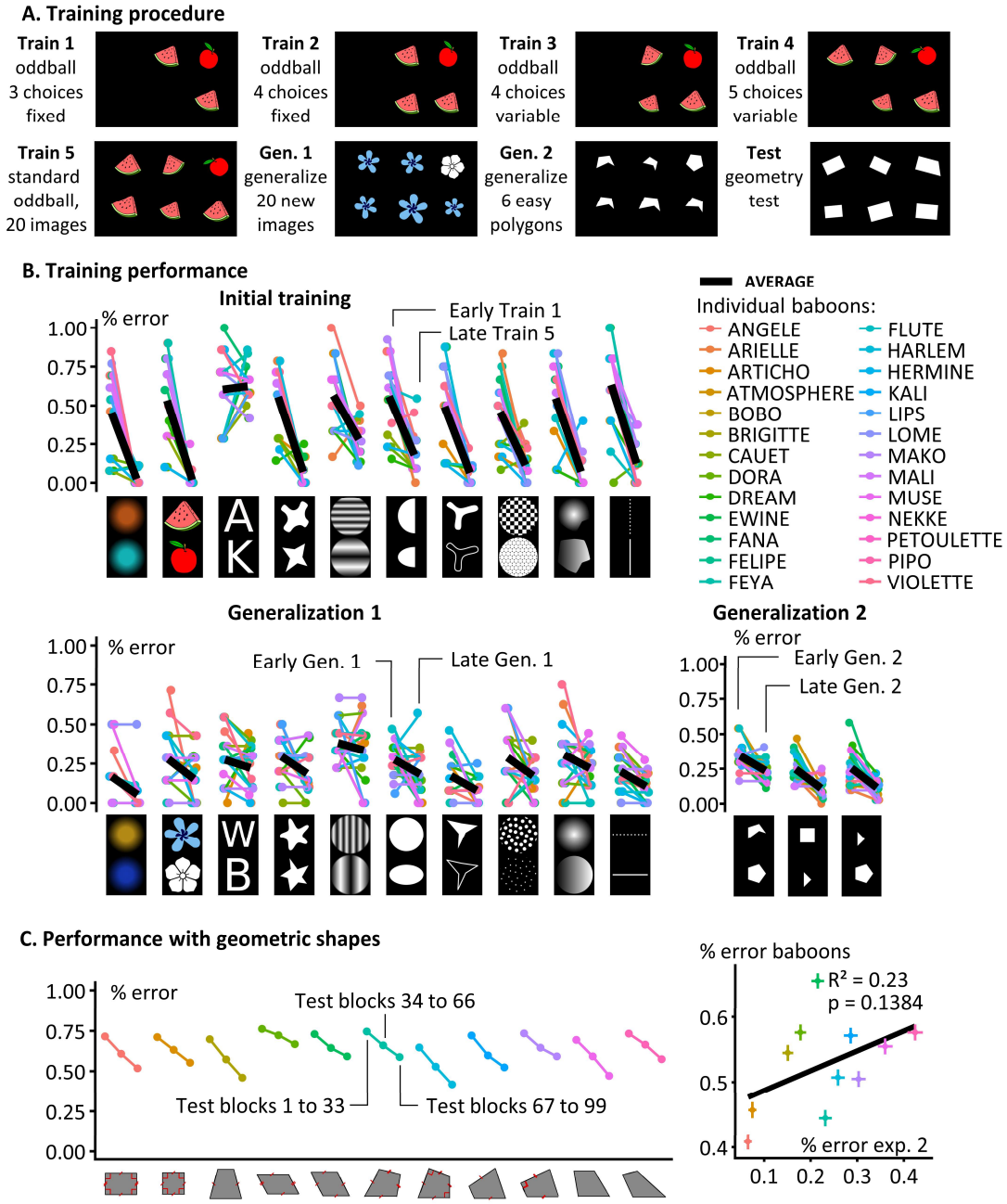
A. Training procedure
Train 1
oddball
3 choices
fixed
Train 2
oddball
4 choices
fixed
Train 3
oddball
4 choices
variable
Train 4
oddball
5 choices
variable
Train 5
standard
oddball,
20 images
Gen. 1
generalize
20 new
images
Gen. 2
generalize
6 easy
polygons
Test
geometry
test
B. Training performance
Initial training
% error
Early Train 1
Late Train 5
AVERAGE
Individual baboons:
ANGELE
ARIELLE
ARTICHO
ATMOSPHERE
BOBO
BRIGITTE
CAUET
DORA
DREAM
EWINE
FANA
FELIPE
FEYA
FLUTE
HARLEM
HERMINE
KALI
LIPS
LOME
MAKO
MALI
MUSE
NEKKE
PETOULETTE
PIPO
VIOLETTE
Generalization 1
Early Gen. 1
Late Gen. 1
Generalization 2
Early Gen. 2
Late Gen. 2
C. Performance with geometric shapes
Test blocks 34 to 66
Test blocks 1 to 33
Test blocks 67 to 99
% error baboons
R² = 0.23
p = 0.1384
% error exp. 2

Figure 3

Figure 4. A double dissociation in geometric shape perception. A, symbolic model. Each shape is coded by a vector of discrete geometric properties (equal angles, parallel sides, equal lengths and right angles; each relationship is assumed to be detected with a tolerance of 12.5%). The distance between the standard and outlier vectors is then used as a predictor of the ease of intruder detection. **B**, neural network model (panel modified from ref. (53), with permission from the authors). CORnet, a model of the ventral visual pathway for image recognition, is used to encode each of the six shapes of a given trial by an activation vector in inferotemporal cortex (IT). The shape whose vector is the most distant ($\mathcal{L}_2$-norm) from the average of the five others, is taken as the network's intruder response. Predicted error rate is obtained by averaging across hundreds of trials. **C,** Simple correlation matrix across shapes between the performance of individual baboons (names in capitals, top rows), the predictions of the two models (middle rows), and various human groups (bottom rows). Color indicates the correlation coefficient *r*. **D,** Standardized regression weights (beta) in a multiple regression of the data from various human and non-human primate groups across 44 data points (11 shapes X 4 outlier types) using the symbolic and neural-network models as predictors. Stars indicate significance level (●, p<.05; *, p<.01; **, p<.001; ***, p<.0001).

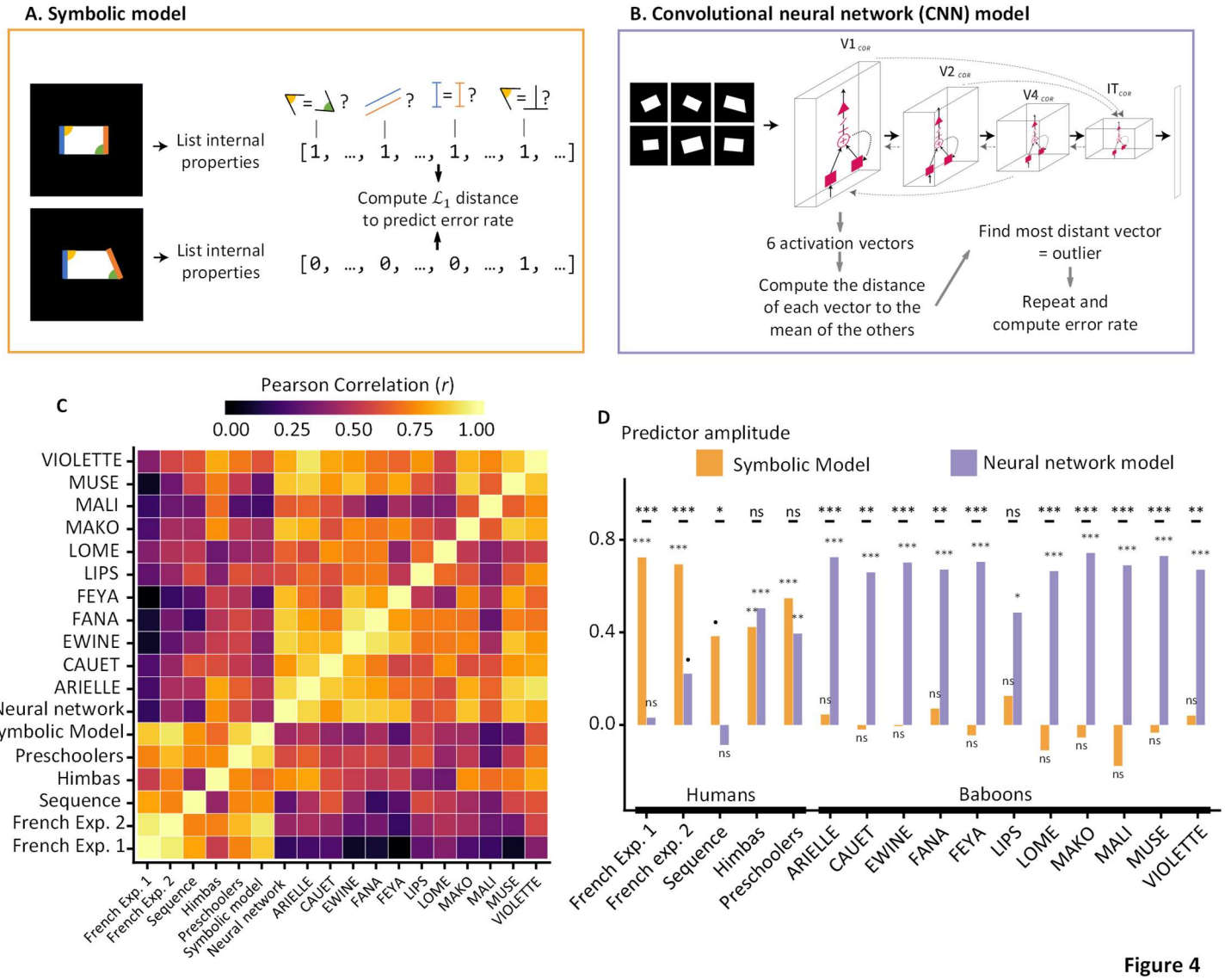
A. Symbolic model
List internal properties
[1, …, 1, …, 1, …, 1, …]
Compute $\mathcal{L}_1$ distance to predict error rate
List internal properties
[0, …, 0, …, 0, …, 1, …]
B. Convolutional neural network (CNN) model
V1 COR
V2 COR
V4 COR
IT COR
6 activation vectors
Compute the distance of each vector to the mean of the others
Find most distant vector = outlier
Repeat and compute error rate
C
Pearson Correlation (r)
0.00 0.25 0.50 0.75 1.00
VIOLETTE
MUSE
MALI
MAKO
LOME
LIPS
FEYA
FANA
EWINE
CAUET
ARIELLE
Neural network
Symbolic Model
Preschoolers
Himbas
Sequence
French Exp. 2
French Exp. 1
D
Predictor amplitude
Symbolic Model
Neural network model
0.8
0.4
0.0
Humans
Baboons
French Exp. 1
French exp. 2
Sequence
Himbas
Preschoolers
ARIELLE
CAUET
EWINE
FANA
FEYA
LIPS
LOME
MAKO
MALI
MUSE
VIOLETTE

Figure 4